© 2018 IJSRSET | Volume 4 | Issue 4 | Print ISSN: 2395-1990 | Online ISSN : 2394-4099
Themed Section : Engineering and Technology

An Efficient Single-Phase Active Device for Power Quality Improvement of Electrified Transportation

Saikrishna Dasari, C. Kullayappa, M. Suresh Kumar
Assistant Professor, PVKKIT, Anantapuram, Andhra Pradesh, India

ABSTRACT

A transformer less hybrid series active filter is proposed to enhance the power quality in single- phase systems with critical loads. This thesis assists the energy management and power quality issues related to electric transportation and focuses on improving electric vehicle load connection to the grid. The control strategy is designed to prevent current harmonic distortions of nonlinear loads to flow into the utility and corrects the power factor of this later. While protecting sensitive loads from voltage disturbances, sags, and swells initiated by the power system, ridded of the series transformer, the configuration is advantageous for an industrial implementation. This polyvalent hybrid topology allowing the harmonic isolation and compensation of voltage distortions could absorb or inject the auxiliary power to the grid. Aside from practical analysis, this thesis also investigates on the influence of gains and delays in the real-time controller stability.

Keywords: Current harmonics, electric vehicle, hybrid series active filter (HSeAF), power quality, real-time control, Fuzzy logic.

I. INTRODUCTION

The forecast of future Smart Grids associated with electric vehicle charging stations has created a serious concern on all aspects of power quality of the power system, while widespread electric vehicle battery charging units [1], [2] have detrimental effects on power distribution system harmonic voltage levels.

On the other hand, the growth of harmonics fed from nonlinear loads like electric vehicle propulsion battery chargers, which indeed have detrimental impacts on the power system and affect plant equipment, should be considered in the development of modern grids. Likewise, the increased rms and peak value of the distorted current waveforms increase heating and losses and cause the failure of the electrical equipment. Such phenomenon effectively reduces system efficiency and should have properly been addressed.

Moreover, to protect the point of common coupling (PCC) from voltage distortions, using a dynamic voltage restorer (DVR) function is advised. A solution is to reduce the pollution of power electronics- based loads directly at their source. Although several attempts are made for a specific case study, a generic solution is to be explored. There exist two types of active power devices to overcome the described power quality issues. The first category are series active filters (SeAFs), including hybrid-type ones. They were developed to eliminate current harmonics produced by nonlinear load from the power system. SeAFs are less scattered than the shunt type of active filters. The advantage of the SeAFs compared to the shunt type is the inferior rating of the compensator versus the load nominal rating.

However, the complexity of the configuration and necessity of an isolation series transformer had decelerated their industrial application in the distribution system. The second category was developed in concern of addressing voltage issues on sensitive loads. Commonly known as DVR, they have a similar configuration as the SeAF [3]. These two categories are different from each other in their control principle. This difference relies on the purpose of their application in the system. The hybrid series active filter (HSeAF) was proposed to address the aforementioned issues with only one combination. Hypothetically, they are capable to compensate current harmonics, ensuring a power factor (PF) correction and eliminating voltage distortions at the PCC. These properties make it an appropriate candidate for power quality investments. The three-phase SeAFs are well documented, whereas limited research works reported the single-phase applications of SeAFs in the literature. In this paper, a single-phase transformer less HSeAF is proposed and capable of cleaning up the grid-side connection bus bar from current harmonics generated by a nonlinear load.

With a smaller rating up to 10%, it could easily replace the shunt active filter. Furthermore, it could restore a sinusoidal voltage at the load PCC.

The advantage of the proposed configuration is that nonlinear harmonic voltage and current producing loads could be effectively compensated. The transformer less hybrid series active filter (THSeAF) is an alternative option to conventional power transferring converters in distributed generation systems with high penetration of renewable energy sources, where each phase can be controlled separately and could be operated independently of other phases.

This thesis shows that the separation of a three-phase converter into single-phase H-bridge converters has allowed the elimination of the costly isolation transformer and promotes industrial application for filtering purposes. The setup has shown great ability to perform requested compensating tasks for the correction of current and voltage distortions, PF correction, and voltage restoration on the load terminal.

The system architecture is introduced in the following section. Then, the operation principle of the proposed configuration is explained. The third section is dedicated to the modeling and analysis of the control algorithm implemented in this work. The dc voltage regulation and its considerations are briefly explained, and the voltage and current harmonic detection method is explicitly described. To evaluate the configuration and the control approach, some scenarios are simulated

II. SYSTEMARCHITECTURE

A. System Configuration

The THSeAF shown in Fig. 1is composed of an H-bridge converter connected in series between the source and the load. A shunt passive capacitor ensures a low impedance path for current harmonics. A dc auxiliary source could be connected to inject power during voltage sags. The dc-link energy storage system is described in. The system is implemented for a rated power of 2200 VA. To ensure a fast transient response with sufficient stability margins over a wide range of operation, the controller is implemented on a dSPACE/dsp1103.

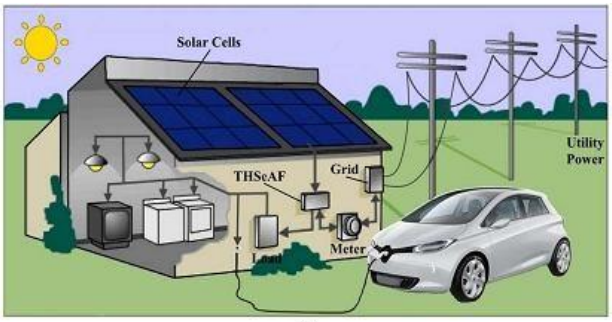

(a)

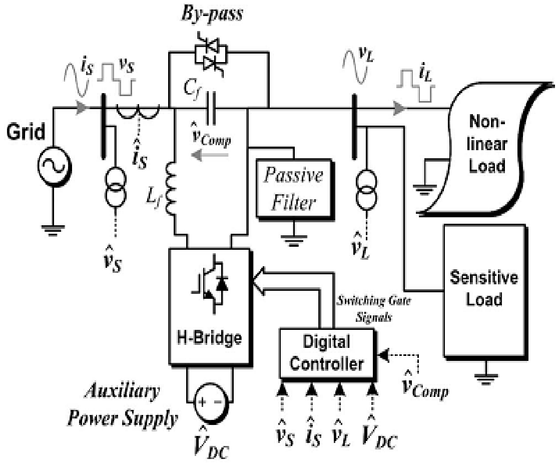

(b)

Figure 1. (a) Schematic of a single-phase smart load with the compensator installation. (b) Electrical diagram of the THSeAF in a single-phase utility.

The system parameters are identified in Table I. A variable source of 120 Vrms is connected to a 1.1- kVA nonlinear load and a 998-VA linear load with a 0.46 PF. The THSeAF is connected in series in order to inject the compensating voltage. On the dc side of the compensator, an auxiliary dc-link energy storage system is installed. Similar parameters are also applied for practical implementation.

Table 1. Configuration Parameters

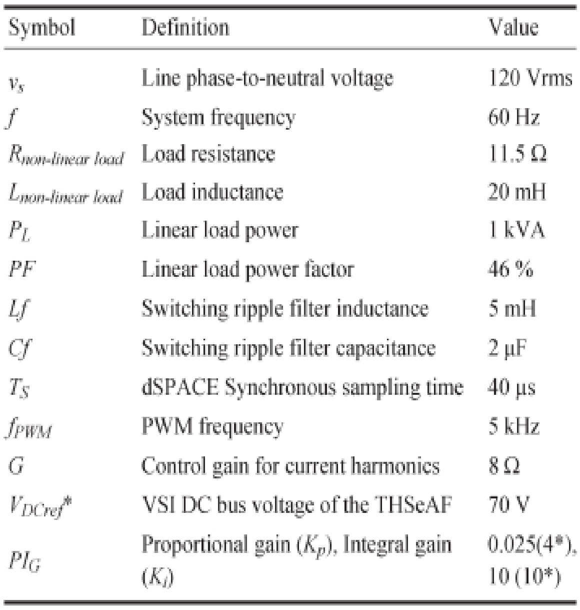

Symbol	Definition	Value
v_s	Line phase-to-neutral voltage	120 Vrms
f	System frequency	60 Hz
$R_{non\text{-}linear\ load}$	Load resistance	11.5 Ω
$L_{non\text{-}linear\ load}$	Load inductance	20 mH
P_L	Linear load power	1 kVA
PF	Linear load power factor	46 %
Lf	Switching ripple filter inductance	5 mH
Cf	Switching ripple filter capacitance	2 µF
T_S	dSPACE Synchronous sampling time	40 µs
f_{PWM}	PWM frequency	5 kHz
G	Control gain for current harmonics	8 Ω
V_{DCref}*	VSI DC bus voltage of the THSeAF	70 V
PI_G	Proportional gain (K_p), Integral gain (K_i)	0.025(4*), 10 (10*)

HSeAFs are often used to compensate distortions of the current type of nonlinear loads. For instance, the distorted current and voltage waveforms of the nonlinear system during normal operation and when the source voltage became distorted are depicted in Figure 2. The THSeAF is bypassed, and current harmonics flowed directly into the grid. As one can perceive, even during normal operation, the current harmonics (with a total harmonic distortion (THD) of 12%) distort the PCC, resulting in a voltage THD of 3.2%. The behavior of the system when the grid is highly polluted with 19.2% of THD is also illustrated.

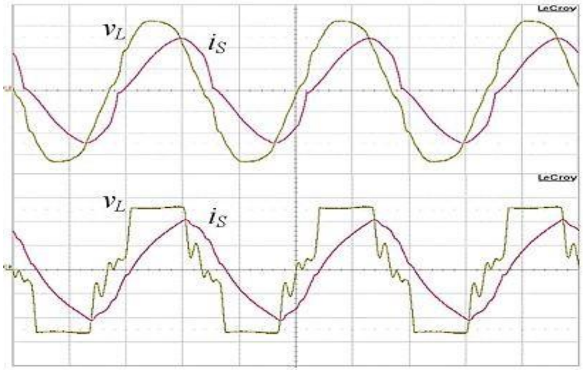

Figure 2. Terminal voltage and current waveforms of the 2-kVA single phase system without compensator. (a) Regular operation. (b) Grid's voltage distortion (scales: 50 V/div for channel 1 and 10 A/div for channel 2).

Table 2. Single-Phase Comparison Of The Thseaf To Prior Hseafs

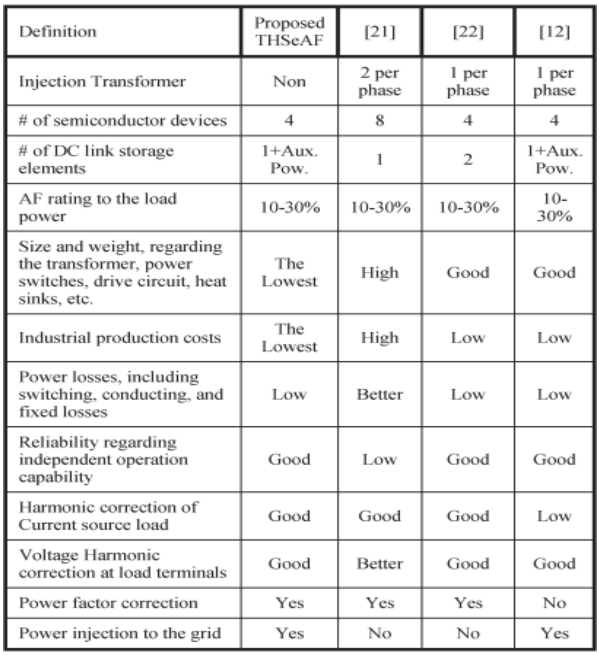

Definition	Proposed THSeAF	[21]	[22]	[12]
Injection Transformer	Non	2 per phase	1 per phase	1 per phase
# of semiconductor devices	4	8	4	4
# of DC link storage elements	1+Aux. Pow.	1	2	1+Aux. Pow.
AF rating to the load power	10-30%	10-30%	10-30%	10-30%
Size and weight, regarding the transformer, power switches, drive circuit, heat sinks, etc.	The Lowest	High	Good	Good
Industrial production costs	The Lowest	High	Low	Low
Power losses, including switching, conducting, and fixed losses	Low	Better	Low	Low
Reliability regarding independent operation capability	Good	Low	Good	Good
Harmonic correction of Current source load	Good	Good	Good	Low
Voltage Harmonic correction at load terminals	Good	Better	Good	Good
Power factor correction	Yes	Yes	Yes	No
Power injection to the grid	Yes	No	No	Yes

The proposed configuration could be solely connected to the grid with no need of a bulky and costly series injection transformer, making this topology capable of compensating source current harmonics and voltage distortion at the PCC. Even if the number of switches has increased, the transformer less configuration is more cost-effective than any other series compensators, which generally uses a transformer to inject the compensation voltage to the power grid. The optimized passive filter is composed of 5th, 7th, and high pass filters. The passive filter should be adjusted for the system upon load and government regulations [4] [5]. A comparison between different existing configurations is given in Table II. It is aimed to point out the advantages and disadvantages of the proposed configuration over the conventional topologies.

To emphasize the comparison table fairly, the equivalent single phase of each configuration is considered in the evaluation. Financial production evaluation demonstrated a 45% reduction in component costs and considerable reduction in assembly terms as well.

B. Operation Principle

The SeAF represents a controlled voltage source (VSI). In order to prevent current harmonics iLh to drift into the source, this series source should present low impedance for the fundamental component and high impedance for all harmonics as shown in Figure 3. The principle of such modeling is well documented in. The use of a well-tuned passive filter is then mandatory to perform the compensation of current issues and maintaining a constant voltage free of distortions at the load terminals. The behavior of the SeAF for a current control approach is evaluated from the phasor's equivalent circuit shown in Figure 3.The nonlinear load could be modeled by a resistance representing the active power consumed and a current source generating current harmonics. Accordingly, the impedance ZL represents the nonlinear load and the inductive load.

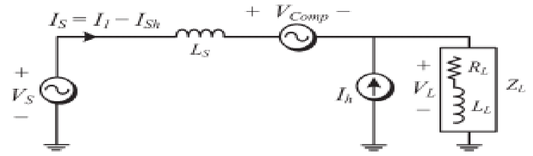

Figure 3. THSeAF equivalent circuit for current harmonics

The SeAF operates as an ideal controlled voltage source (Vcomp) having a gain (G) proportional to the current harmonics (Ish) flowing to the grid (Vs)

$$V_{\text{comp}} = G.I_{sh} - V_{Lh}. \tag{1}$$

This allows having individual equivalent circuit for the fundamental and harmonics

$$V_{\text{source}} = V_{s1} + V_{sh}, \qquad V_L = V_{L1} + V_{Lh}. \tag{2}$$

The source harmonic current could be evaluated

$$V_{sh} = -\, Z_s.I_{sh} + V_{\text{comp}} + V_{Lh} \tag{3}$$

$$V_{Lh} = Z_L(I_h - I_{sh}). \tag{4}$$

Combining (3) and (4) leads to (5)

$$I_{sh} = \frac{V_{sh}}{(G - Z_s)}. \tag{5}$$

If gain G is sufficiently large (G→∞), the source current will become clean of any harmonics (Ish→0). This will help improve the voltage distortion at the grid side. In this approach, the THSeAF behaves as high-impedance open circuit for current harmonics, while the shunt high-pass filter tuned at the system frequency creates a low-impedance path for all harmonics and open circuit for the fundamental; it also helps for PF correction.

III. MODELING AND CONTROL OF THE SINGLE- PHASE THSeAF

A. Average and Small-Signal Modeling

Based on the average equivalent circuit of an inverter, the small-signal model of the proposed configuration can be obtained as in Fig. 4. Here after, d is the duty cycle of the upper switch during a switching period, whereas¯ v and ¯I denote the average values in a switching period of the voltage and current of the same leg. The mean converter output voltage and current are expressed by (6) and (7) as follows:

$$\bar{v}_O = \underbrace{(2d-1)} V_{\text{DC}} \tag{6}$$

where the (2d−1) equals tom, then

Calculating the Thevenin equivalent circuit of the harmonic current source leads to the following assumption:

$$\bar{v}_h(j\omega) = \frac{-j\bar{i}_h}{C_{HPF} \cdot \omega_h}. \qquad (8)$$

If the harmonic frequency is high enough, it is possible to assume that there will be no voltage harmonics across the load. The state-space small-signal ac model could be derived by a linearized perturbation of the averaged model as follows:

$$\dot{x} = Ax + Bu. \qquad (9)$$

Hence, we obtain

$$\frac{d}{dt}\begin{bmatrix} \bar{v}_{Cf} \\ \bar{v}_{CHPF} \\ \bar{i}_S \\ \bar{i}_f \\ \bar{i}_L \end{bmatrix} = \begin{bmatrix} 0 & 0 & \frac{1}{C_f} & \frac{1}{C_f} & 0 \\ 0 & 0 & \frac{1}{C_{HPF}} & 0 & -1/C_{HPF} \\ -1/L_S & -1/L_S & -r_c/L_S & -r_c/L_S & 0 \\ -1/L_f & 0 & -r_c/L_f & -r_c/L_f & 0 \\ 0 & \frac{1}{L_L} & 0 & 0 & -R_L/L_L \end{bmatrix}$$

$$\times \begin{bmatrix} \bar{v}_{Cf} \\ \bar{v}_{CHPF} \\ \bar{i}_S \\ \bar{i}_f \\ \bar{i}_L \end{bmatrix} + \begin{bmatrix} 0 & 0 & 0 \\ 0 & 0 & 0 \\ \frac{1}{L_S} & 0 & \frac{1}{L_S} \\ 0 & \frac{m}{L_f} & 0 \\ 0 & 0 & -1/L_L \end{bmatrix} \times \begin{bmatrix} \bar{v}_S \\ V_{\mathrm{DC}} \\ \bar{v}_h \end{bmatrix}. \qquad (10)$$

Moreover, the output vector is

$$y = Cx + Du \qquad (11)$$

Or

$$\begin{bmatrix} \bar{v}_{\mathrm{comp}} \\ \bar{v}_L \end{bmatrix} = \begin{bmatrix} 1 & 0 & r_c & r_c & 0 \\ 0 & 1 & 0 & 0 & 0 \end{bmatrix} \times \begin{bmatrix} \bar{v}_{Cf} \\ \bar{v}_{CHPF} \\ \bar{i}_S \\ \bar{i}_f \\ \bar{i}_L \end{bmatrix}$$

$$+ \begin{bmatrix} 0 & 0 & 0 \\ 0 & 0 & -1 \end{bmatrix} \times \begin{bmatrix} \bar{v}_S \\ V_{\mathrm{DC}} \\ \bar{v}_h \end{bmatrix}. \qquad (12)$$

$$\bar{i}_{\mathrm{DC}} = m\bar{i}_f. \qquad (7)$$

By means of (10) and (12), the state-space representation of the model is obtained as shown in Figure 4.

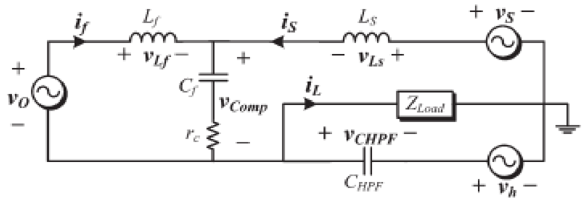

Figure 4. Small-signal model of transformer less HSeAF in series between the grid and the load.

The transfer function of the compensating voltage versus the load voltage, TV_CL(s), and the source current, TCI(s), are developed in the Appendix. Meanwhile, to control the active part independently, the derived transfer function should be autonomous from the grid configuration. The transfer function TVm presents the relation between the output voltages of the converter versus the duty cycle of the first leg converter's upper switch

$$T_V(s) = \frac{V_{\mathrm{comp}}}{V_O} = \frac{r_C C_f s + 1}{L_f C_f s^2 + r_C C_f s + 1} \qquad (13)$$

$$T_{Vm}(s) = \frac{V_{\mathrm{comp}}}{m} = V_{DC} \cdot T_V(s). \qquad (14)$$

The further detailed derivation of steady-state transfer functions is described in Section V. A dc auxiliary source should be employed to maintain an adequate supply on the load terminals. During the sag or swell conditions, it should absorb or inject power to keep the voltage magnitude at the load terminals within a specified margin [6]. However, if the compensation of sags and swells is less imperative, a capacitor could be deployed. Consequently, the dc-link voltage across the capacitor should be regulated as demonstrated in Figure 5.

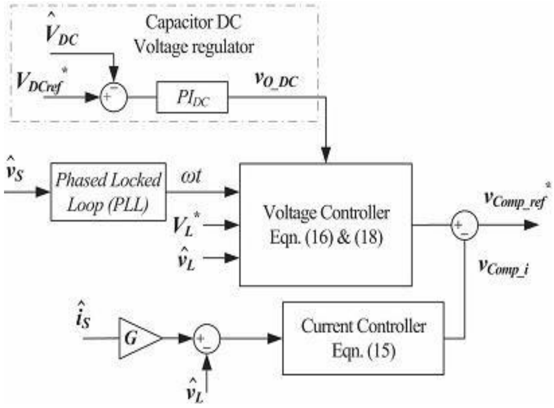

Figure 5. Control system scheme of the active part.

B. Voltage and Current Harmonic Detection

The outer-loop controller is used where a capacitor replaces the dc auxiliary source. This control strategy is well explained in the previous section. The inner-loop control strategy is based on an indirect control principle. A fast Fourier transformation was used to extract the magnitude of the fundamental and its phase degree from current harmonics.

The control gain G representing the impedance of the source for current harmonics has a sufficient level to clean the grid from current harmonics fed through the nonlinear load.

The second proportional integrator (PI) controller used in the outer loop was to enhance the effectiveness of the controller when regulating the dc bus. Thus, a more accurate and faster transient response was achieved without compromising the compensation behavior of the system. According to the theory, the gain G should be kept in a suitable level, preventing the harmonics from flowing into the grid. As previously discussed, for a more precise compensation of current harmonics, the voltage harmonics should also be considered. The compensating voltage for current harmonic compensation is obtained from

$$v_{\text{comp\_}i}(t) = (-G\hat{i}_S + \hat{v}_L) - [| - Gi_{S1} + v_{L1}| \cdot \sin(\omega_S t - \theta)]. \tag{15}$$

Hereby, as voltage distortion at the load terminals is not desired, the voltage sag and swell should also be investigated in the inner loop. The closed-loop equation (16) allows to indirectly maintaining the voltage magnitude at the load side equal to V∗L as a predefined value, within acceptable margins

$$v_{\text{comp\_}v} = \hat{v}_L - V_L^* \sin(\omega_S t). \tag{16}$$

The entire control scheme for the THSeAF presented in Figure 5was used and implemented in MATLAB/Simulink for real-time simulations and the calculation of the compensating voltage. The real-time toolbox of d-SPACE was used for compilation and execution on the dsp-1103 control board. The source and load voltages, together with the source current, are considered as system input signals. According to Srianthumrong et al. [7] [8], an indirect control increases the stability of the system.

The source current harmonics are obtained by extracting the fundamental component from the source current

$$v^*_{\text{com\_ref}} = v_{\text{comp\_}v} - v_{\text{comp\_}i} + v_{\text{DC\_}ref} \tag{17}$$

where the vDC_ref is the voltage required to maintain the dc bus voltage constant

$$v_{\text{DC\_}ref}(t) = V_{O\_\text{DC}} \cdot \sin(\omega_S t). \tag{18}$$

A phase-locked loop was used to obtain the reference angular frequency (ωs). Accordingly, the extracted current harmonic contains a fundamental component synchronized with the source voltage in order to correct the PF. This current represents the reactive power of the load. The gain G representing the resistance for harmonics converts current into a relative voltage. The generated reference voltage vcomp_i required to clean the source current from harmonics is described in (15).

According to the presented detection algorithm, the compensated reference voltage v∗Comp_ref is calculated. Thereafter, the reference signal is compared with the measured output voltage and applied to a PI controller to generate the corresponding gate signals as in Figure 6.

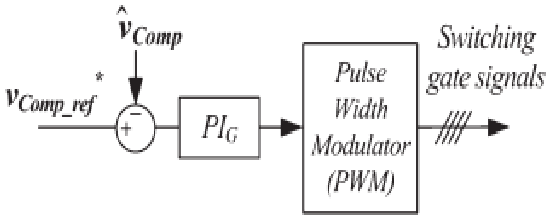

Figure 6. Block diagram of THSeAF and PI controller.

C. Stability Analysis for Voltage and Current Harmonics

The stability of the configuration is mainly affected by the introduced delay of a digital controller. This section studies the impact of the delay first on the inclusive compensated system according to works cited in the literature [9]. Thereafter, its effects on the active compensator is separated from the grid. Using purely inductive source impedance (see Fig. 4) and Kirchhoff's law for harmonic frequency components,(19) is derived. The delay time of the digital controller, large gain G, and the high stiffness of the system seriously affect the stability of the closed-loop controlled system

$$I_{sh}(s) = \frac{V_{sh} - V_{\text{Comp}} - V_{Lh}}{L_s s}. \tag{19}$$

The compensating voltage including the delay time generated by the THSeAF in the Laplace domain [see (1)] is

$$v_{\text{Comp}} = G \cdot I_{sh} \cdot e^{-\tau s} - V_{Lh}. \tag{20}$$

Considering (19) and (20), the control diagram of the system with delay is obtained as in Figure 7.

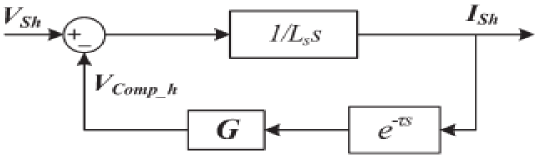

Figure 7. Control diagram of the system with delay.

For the sake of simplicity, the overall delay of the system is assumed to be a constant value τ. Therefore, the open-loop transfer function is obtained

$$G(s) = \frac{G}{L_s s} e^{\tau s}. \qquad (21)$$

From the Nyquist stability criterion, the stable operation of the system must satisfy the following condition:

$$G < \frac{\pi L_s}{2\tau}. \qquad (22)$$

A system with a typical source inductance Ls of 250µH and a delay of 40µs is considered stable according to when the gain G is smaller than 10Ω. Experimental results confirm the stability of the system presented in this thesis [10]. Moreover, the influence of the delay on the control algorithm should also be investigated. According to the transfer functions (13) and (14), the control of the active part is affected by the delay introduce by the digital controller. Thus, assuming an ideal switching characteristic for the IGBTs, the closed-loop system for the active part controller is shown in Fig. 8.

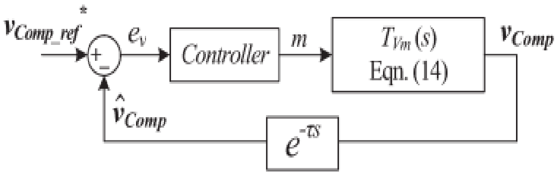

Figure 8. Closed-loop control diagram of the active filter with a constant delay time τ.

The open-loop transfer function in Fig. 8turns to (23), where the τ is the delay time initiated by the digital controller

$$F(s) = PI_G \cdot T_{V_m} \cdot e^{\tau s} = \frac{(r_C C_f V_{DC} s + V_{DC}) \cdot (K_p s + K_i) e^{\tau s}}{s \cdot (L_f C_f s^2 + r_C C_f s + 1)}. \qquad (23)$$

A PI controller with system parameters described in Table I demonstrates a smooth operation in the stable region. By means of MATLAB, the behavior of the system's transfer function F(s)is traced in Fig. 9. The root locus and the Bode diagram of the compensated open-loop system demonstrate a gain margin of 8.06 dB and a phase margin of 91◦.

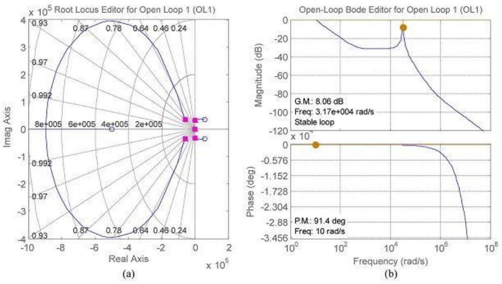

Figure 9. Compensated open-loop system with delay time of 40µs. (a) Root locus diagram. (b) Bode diagram.

IV. SIMULATION RESULTS

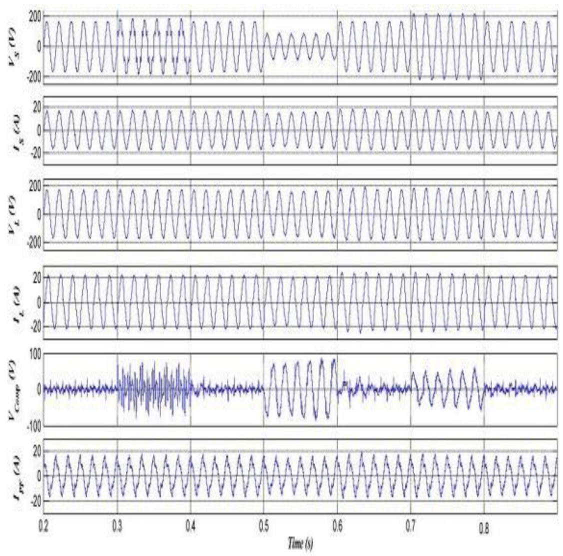

Figure 11. Simulation of the system with the THSeAF compensating current harmonics and voltage egulation. (a) Source voltagevS, (b) source currentiS, (c) load voltage vL, (d) load current iL, (e) active-filter voltage VComp, and (f) harmonics current of the passive filter iPF.

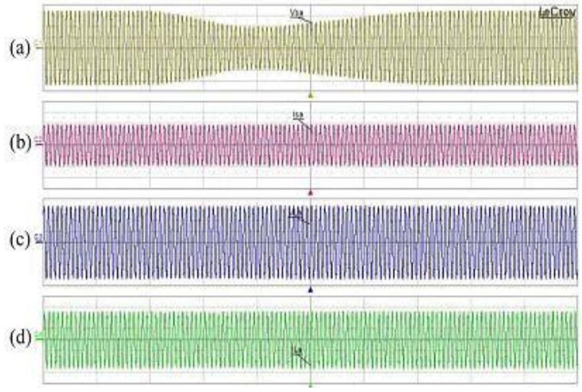

Figure 12. Waveforms during a variation of the source voltage. (a) Source voltagevS[50 V/div], (b) source current iS[10 A/div], (c) load PCC voltagevL[50 V/div], and (d) load current iL[10 A/div].

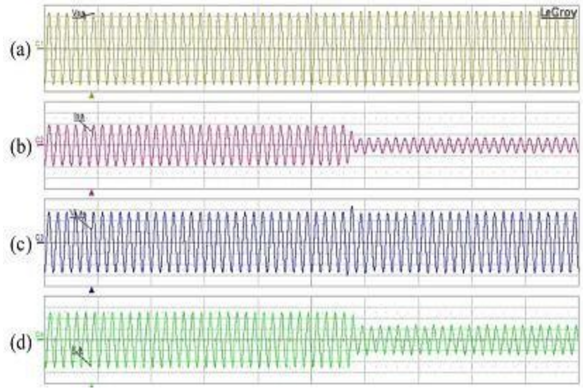

Figure 13. Waveforms during a dynamic load variation. Source voltagevS[50 V/div], (b) source currentiS[10 A/div], (c) load PCC voltage vL[50 V/div], and (d) load current iL[10 A/div].

V. CONCLUSION

In this thesis, a transformer less HSeAF for power quality improvement was developed and tested. The thesis highlighted the fact that, with the ever increase of nonlinear loads and higher exigency of the consumer for a reliable supply, concrete actions should be taken into consideration for future smart grids in order to smoothly integrate electric car battery chargers to the grid. The key novelty of the proposed solution is that the proposed configuration could improve the power quality of the system in a more general way by compensating a wide range of harmonics current, even though it can be seen that the THSeAF regulates and improves the PCC voltage. Connected to a renewable auxiliary source, the topology is able to counteract actively to the power flow in the system.

This essential capability is required to ensure a consistent supply for critical loads. Behaving as high-harmonic impedance, it cleans the power system and ensures a unity PF.

The theoretical modeling of the proposed configuration was investigated. The proposed transformer less configuration was simulated and experimentally validated. It was demonstrated that this active compensator responds properly to source voltage variations by providing a constant and distortion-free supply at load terminals. Furthermore, it eliminates source harmonic currents and improves the power quality of the grid without the usual bulky and costly series transformer.

VI. REFERENCES

[1]. L. Jun-Young and C. Hyung-Jun, "6.6-kW onboard charger design using DCM PFC converter with harmonic modulation technique and two-stage dc/dc converter,"IEEE Trans. Ind. Electron., vol. 61, no. 3, pp. 1243-1252, Mar. 2014.

[2]. R. Seung-Hee, K. Dong-Hee, K. Min-Jung, K. Jong-Soo, and L. ByoungKuk, "Adjustable frequency duty-cycle hybrid control strategy for fullbridge series resonant converters in electric vehicle chargers," IEEE Trans. Ind. Electron., vol. 61, no. 10, pp. 5354-5362, Oct. 2014.

[3]. P. T. Staats, W. M. Grady, A. Arapostathis, and R.S. Thallam, "A statistical analysis of the effect of electric vehicle battery charging on distribution system harmonic voltages," IEEE Trans. Power Del., vol. 13, no. 2, pp. 640-646, Apr. 1998.

[4]. A. Kuperman, U. Levy, J. Goren, A. Zafransky, and A. Savernin, "Battery charger for electric

vehicle traction battery switch station,"IEEE Trans. Ind. Electron., vol. 60, no. 12, pp. 5391-5399, Dec. 2013.

[5]. Z. Amjadi and S. S. Williamson, "Modeling, simulation, control of an advanced Luo converter for plug-in hybrid electric vehicle energy-storage system,"IEEE Trans. Veh. Technol., vol. 60, no. 1, pp. 64-75, Jan. 2011.

[6]. H. Akagi and K. Isozaki, "A hybrid active filter for a three-phase 12-pulse diode rectifier used as the front end of a medium-voltage motor drive," IEEE Trans. Power Del., vol. 27, no. 1, pp. 69-77, Jan. 2012.

[7]. A. F. Zobaa, "Optimal multiobjective design of hybrid active power filters considering a distorted environment, "IEEE Trans. Ind. Electron., vol. 61, no. 1, pp. 107-114, Jan. 2014.

[8]. D. Sixing, L. Jinjun, and L. Jiliang, "Hybrid cascaded H-bridge converter for harmonic currentcompensation,"IEEE Trans. Power Electron., vol. 28, no. 5, pp. 2170-2179, May 2013.

[9]. M. S. Hamad, M. I. Masoud, and B. W. Williams, "Medium-voltage 12-pulse converter: Output voltage harmonic compensation using a series APF,"IEEE Trans. Ind. Electron., vol. 61, no. 1, pp. 43-52, Jan. 2014.

[10]. J. Liu, S. Dai, Q. Chen, and K. Tao, "Modelling and industrial application of series hybrid active power filter,"IET Power Electron., vol. 6, no. 8, pp. 1707- 1714, Sep. 2013.